EXPLORING ADIPOSE BIOLOGY IN ZEBRAFISH

by

Madhukar Aryal

A thesis submitted to the faculty of
The University of Utah
in partial fulfillment of the requirements for the degree of

Master of Science

Department of Biochemistry

The University of Utah

December 2014

The University of Utah Graduate School

STATEMENT OF THESIS APPROVAL

The thesis of **Madhukar Aryal**

has been approved by the following supervisory committee members:

Amnon Schlegel	, Chair	**08/07/2014** Date Approved
Janet E. Lindsley	, Member	**08/07/2014** Date Approved
Claudio J. Villanueva	, Member	**08/07/2014** Date Approved

and by **Wesley L. Sundquist** , Chair/Dean of

the Department/College/School of **Biochemistry**

and by David B. Kieda, Dean of The Graduate School.

ABSTRACT

Adipose tissue plays a key role in metabolic homeostasis. Adipose tissue functions are associated with various pathological conditions including obesity, insulin resistance, and other metabolic complications. Understanding the normal regulation of adipose tissue formation and homeostasis is imperative to understanding the pathologies associated with a decrease or increase in adipose tissue. We have undertaken an unbiased forward genetic screening to identify novel genes that affect lipid storage in zebrafish adipose tissue. We aimed to clone and characterize gene(s) responsible for *sans suet (sns)* mutant. We utilized next generation sequencing analysis and obtained four candidate variants that may have genetic linkage with *sns* mutation. The targeted sequencing revealed that the candidate variant on chromosome 5 (*hdr* gene) was heterozygous in *sns* mutant fish. We hypothesize that the region near the *hdr* gene may have a stretch of a homozygous region that may be linked to *sns* phenotype. In addition, our goal was to develop transgenic reporter and molecular tools to manipulate gene function for the study of adipose biology in zebrafish. We aimed to create a transgenic reporter line that expresses mCherry exclusively in adipocytes. While testing the nuclease activity of Transcription Activator Like-Effector Nuclease (TALEN) *in vivo*, we found the inefficient introduction of double strand breaks in the predefined site of the genome. This result necessitates redesigning the genome engineering nuclease for efficient double strand breakage for successful knock-in.

TABLE OF CONTENTS

LIST OF FIGURES

CHAPTER 1

POSITIONAL CLONING AND MAPPING OF *SAN SUET* MUTATION

1.1 Introduction

Lipid storage is an evolutionary conserved process that occurs from yeast to higher vertebrates. In yeast, lipids are stored as droplets composed surface monolayer of phospholipids that surround hydrophobic lipid cores (1). Nematodes such as *Caenorhabiditis elegans* (*C. elegans*) adults store lipids in gut granules and enterocyte lysosomes. *Drosophila* consists of specialized fat bodies to store lipids (2). The vertebrates possess the specialized adipose tissues to store lipids in the body. The adipocyte functions extend beyond passive energy storage, in that they have endocrine secretory properties and provide mechanical protection to the body (3). White adipose tissue (WAT) is characterized by a large unilocular lipid droplet that stores the bulk of neutral lipids. WAT regulates various processes such as insulin sensitivity, lipid metabolism, and satiety (4).

The rapid rise in prevalence of obesity and its associated complications such as obesity, insulin resistance, diabetes, and cardiovascular diseases have posed a major financial burden to tackle and prevent these conditions worldwide (4). The deranged lipid storage in adipose tissue is associated with a variety of these clinical conditions. Therefore, it demands special attention to study the adipose tissue formation, homeostasis

and lipid storage *in vivo* and the pathologies associated with it.

1.1.1 Mechanism of adipogenesis

Adipocytes are derived from pluripotent mesenchymal stem cells that reside in vascular stroma of adipose tissues. Under appropriate signal, these stem cells are stimulated and committed to form pre-adipocyte lineage. These pre-adipocytes undergo mitotic clonal expansion and differentiation to mature adipocytes (5). The developmental programs, transcriptional cascades, and basic proteins that regulate adipocyte development, fat synthesis, storage, and lipolysis are functionally conserved (6).

Multiple signaling pathways have been implicated in normal adipogenesis, including the bone morphogenetic protein (BMPs), transforming growth factor- beta (TGF-β), insulin like growth factor 1 (IGF-1), fibroblast growth factor (FGF), wingless/integration1 (Wnt), and hedgehog (HH) signaling pathways. Genetic alterations of these signaling pathways have shown to influence adipose tissue depots (3). During the transformation of mature adipocytes, pre-adipocytes undergo marked changes in morphology and gene expression. Peroxisome proliferator-activated receptor gamma (PPAR-γ) is the master transcriptional factor that is necessary and sufficient to drive adipogenesis (7). PPAR-γ activates its targets in pre-adipocytes and adipocytes, including CCAAT/enhancer-binding protein alpha (C/EBP-α). C/EBP-α, in turn, activates PPAR-γ via a positive feedback loop. PPAR-γ and C/EBP-α also activate expression of genes in lipid metabolism, glucose transport, fatty acid handling, and secretory factors such as adiponectin and leptin (3, 8).

1.1.2 Lipid storage and mobilization in adipose tissue

Adipose tissue is the major site for storage of surplus fuels in the form of triglycerides (neutral lipid) in the body. However, when the fuels are scarce, adipose tissue undergo breakdown of stored triglycerides into fatty acids and glycerol. The fatty acids enter the bloodstream and mobilize to various organs for oxidation. Glycerol is transported into the liver, where it serves as gluconeogenic substrate. The lipid synthesis and mobilization processes in adipose tissues are regulated by different hormones and nutrients. Insulin enhances uptake and storage of lipids in adipose tissues. In response to adrenergic signals, phosphorylation and activation hormone sensitive lipase lead to hydrolysis of stored triglycerides into free fatty acid and glycerol in adipose tissue (Fig. 1.1).

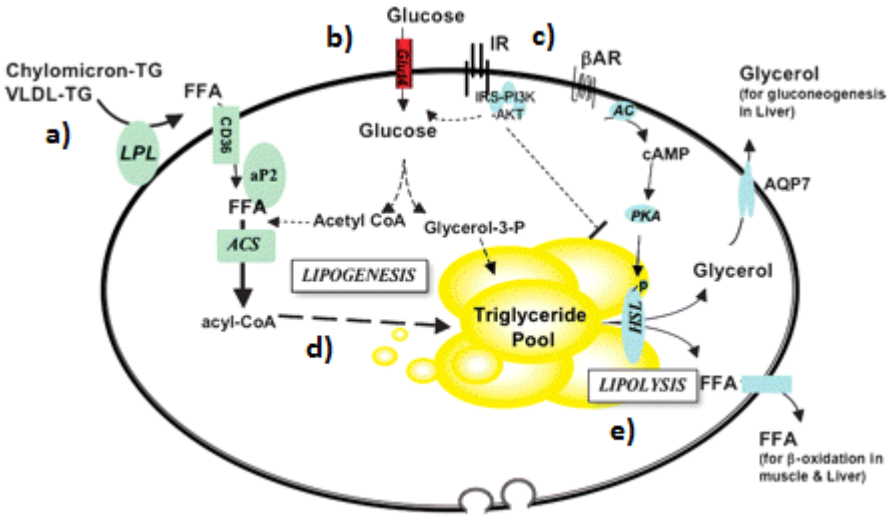

Figure 1.1 Lipid Metabolism in adipose tissue. a) Uptake of fatty acids from circulation and conversion into acyl CoA. b) Uptake of glucose and conversion to acetyl coA, precursor for fatty acids, c) Regulation of triglyceride metabolism by insulin and adrenergic signals, d) synthesis and incorporation of triglycerides into lipid droplets, e) breakdown of lipids and release of fatty acid and glycerol to circulation (*(9)*). Abbreviations: triglycerides (TG), very low density lipoprotein (VLDL), free fatty acids (FFA), Acyl CoA synthetase (ACS), insulin receptor (IR), insulin receptor substrate (IRS), phosphoinositide-3-kinase (PI3K), adenylate cyclase (AC), cyclic adenosine monophosphate (cAMP), protein kinase A (PKA), hormone sensitive lipase (HSL).

The dietary and endogenous lipids are transported as lipoproteins in the blood stream. Chylomicrons and very low density lipoprotein (VLDL) consist of a large proportion of triglycerides. The lipoprotein lipase facilitates the import of fatty acid import into adipose tissues. The lipoprotein lipase hydrolyzes triglycerides into fatty acid and glycerol. The fatty acid are taken into adipocytes and converted into fatty acyl CoA and ultimately into triglycerides that are incorporated into lipid droplets. The glucose can be metabolized into pyruvate, which can be further oxidized to acetyl CoA. Acetyl CoA is the precursor for de novo fatty acid synthesis and triglyceride synthesis (9).

1.1.3 Influence of fatty acid metabolism in adiposity

Genome-wide and targeted screens have been performed in yeast, worms, flies, mice, and human cell lines to identify the genes that influence degree of adiposity (10–14). These studies have contributed to our current understanding of adipose biology and lipid metabolism. Studies have shown that defects in processes such as fatty acid synthesis, desaturation, elongation, or fatty acid oxidation result in decreased lipogenesis, decreased lipid storage, increased fatty acid oxidation, and resistance to diet induced insulin resistance (15–17). Mice lacking acetyl CoA carboxylase 2, an enzyme involved in de novo fatty acid synthesis, showed increased fatty acid oxidation, energy expenditure, and decreased adiposity (15). Similarly, mice lacking *ELOVL2* are reported to have constrained lipid storage. These mice have normal food intake but increased fatty acid oxidation (16).

Impaired lipid uptake from the intestine may influence adiposity. The zebrafish fat-free (*ffr*) mutants have impaired absorption of lipid from intestine. The

characterization of *ffr* revealed the altered vesicular transport resulting in impaired lipid absorption in the enterocytes (18).

1.1.4 Influence of feeding regulation in adiposity

The hypothalamus-adipose axis plays a key role in controlling food intake and appetite. The arcuate neurons release orixgenic neuropeptides such as neuropeptide Y (NPY) and Agouti related protein (AgRP), which increase the food intake (19). The anorexigenic hormone proopiomelanocorticotrophin (POMC) decreases the food intake. Leptin released from adipose tissue binds to the leptin receptor in the arcuate nucleus, resulting in increased expression of POMC and decreased food intake. Impaired genes that affect hypothalamus-adipose control of feeding alter energy intake and adiposity in animals (19–22).

1.1.5 Lipodystrophy genes and adiposity

Lipodystrophies are a group of rare disorders that are marked by selective loss of adipose depots. Lipodystrophies predispose patients to metabolic complications such as insulin resistance, hypertriglyceridemia, and hepatic steatosis (23). Lipodystrophies can be classified as a genetic and acquired form. Disruption of key genes involved in adipogenesis, lipid uptake, synthesis, and lipid droplet formation lead to the genetic form of lipodystrophies in humans. The genetic form of lipodystrophy can be classified into familial partial lipodystrophy (FPLD) and congenital partial lipodystrophy (CGL). Mutation in genes such as *PPAR-γ*, laminA/C (*LMNA*), *AKT2*, and perilipin (*PLIN1*) are reported in FPLD. Mutation in 1-acylglycerol-3-phosphate-O-actyl transferase-2

(*AGPAT2*), *Berardinell—Seip congenital lipodystrophy 2* (*BCSL2*), *Caveolin 1* (*CAV1*), and *Polymerase I and transcript release factor* (*PTRF*) are reported in CGL (23). These evidences indicate that lipodystrophies are a heterogeneous group of disorders. The underlying mechanism of disease depends on the type of gene that is mutated, which adds complexity to designing targeted treatments (23).

1.1.6 Zebrafish as a model to study lipid metabolism

Zebrafish are an established model for studying vertebrate development and organogenesis (24). Forward genetics in zebrafish provided meaningful insight into these processes (25). The development of a transgenic reporter and genetic tools offered zebrafish as a tractable system to perform large genetic screens and chemical screens (25). Our laboratory focuses on lipid metabolism and abnormal lipid storage using a novel zebrafish model system. The inherent ability of zebrafish to develop obesity and atherosclerosis on high calorie diets, the presence of *cholesterol ester transfer proteins* (*CETP*) ortholog, and the presence of lipoprotein abundance similar to humans highlights the zebrafish (*Danio rerio*) as an attractive model to study lipid metabolism and associated disorders (26).

1.1.7 Adipogenesis in zebrafish

Adipogenesis in zebrafish occurs after 8 days postfertilization (dpf). Pancreatic and visceral white adipose tissue are seen at approximately 8 to 10 dpf. Developmental timing of adipose tissue is asynchronous in zebrafish (27, 28). Adipogenesis in zebrafish occurs at the larval stage, and WAT is the only type of adipose tissue present. The

semitransparent zebrafish larvae provide unique opportunity to study ontogeny of adipogenesis. WAT size in zebrafish is responsive to diet, starvation, and chemicals (27), (29). Zebrafish WATs also expresses adipocyte-specific genes (*fabp11a*, *cfd,* and *adipoq*), and they are functionally conserved to higher vertebrates (27, 28). This evidence supports the notion that zebrafish are a simple vertebrate system to study adipose biology.

1.1.8 Metamorphosis in zebrafish

Metamorphosis is an abrupt postembryonic transformation of larvae to juvenile fish. Thyroid hormones trigger the metamorphosis via binding to the thyroid receptor (TR) protein. In zebrafish, the release of thyroid hormone occurs in a pulsatile manner. Thyroxine (T_3), the active form of thyroid hormone, rises at 4 to 5 dpf and peaks at 10 dpf. A second pulse begins at 14 dpf, peaks at 21 dpf, and starts declining after approximately 29 dpf (30). Thyroid hormone binding to TR triggers metamorphosis and directly regulates a few subsets of early response genes that in turn activate large secondary target genes in different organs (31). A variety of larval traits (fins, skins, melanophores, digestive system, and sensory system) are remodeled in a coordinated manner to generate adult zebrafish (32). The process involves tissue resorption, patterning, and redistribution. Studies in *Drosophila* showed that fat bodies (analogous to adipose tissues of vertebrate) undergo extensive redistribution, remodeling, apoptosis, and regeneration during metamorphosis (33). It is not known whether metamorphosis influences adipose tissue formation, survival, and remodeling in zebrafish and higher vertebrates.

1.1.9 Forward genetic screen and genetic mapping

Forward genetic approaches seek to identify genes involved in the biological pathway or process through screening the particular displayed phenotype in mutagenized animals. N-ethyl-N-Nitrosourea (ENU) is a chemical mutagen that is standard choice for random mutagenesis. ENU is an alkylating agent that can achieve high random mutagenesis in zebrafish premeiotic germ cells. The subsequent mapping of the allele within the genome reveals genes that are associated with the observed biological process. Various markers such as simple sequence length polymorphisms (SSLPs) and single nucleotide polymorphisms (SNPs) have been previously used to establish linkage (34). Mapping is based on the probability of recombination events occurring in a diploid genome during meiosis. A marker that is tightly linked to the mutation will segregate with the phenotype. In contrast, unlinked markers will segregate independently of the trait. Alternatively, genome sequencing technology has emerged as a robust method for positional cloning. Genome sequencing technologies have been applied to find linkage in different model organisms, including zebrafish (35–41).

1.2 Materials and Methods

1.2.1 ENU mutagenesis and recovery of mutants

The standard ENU mutagenesis was performed as previously described (42). The breeding scheme is described in (Fig. 1.2).

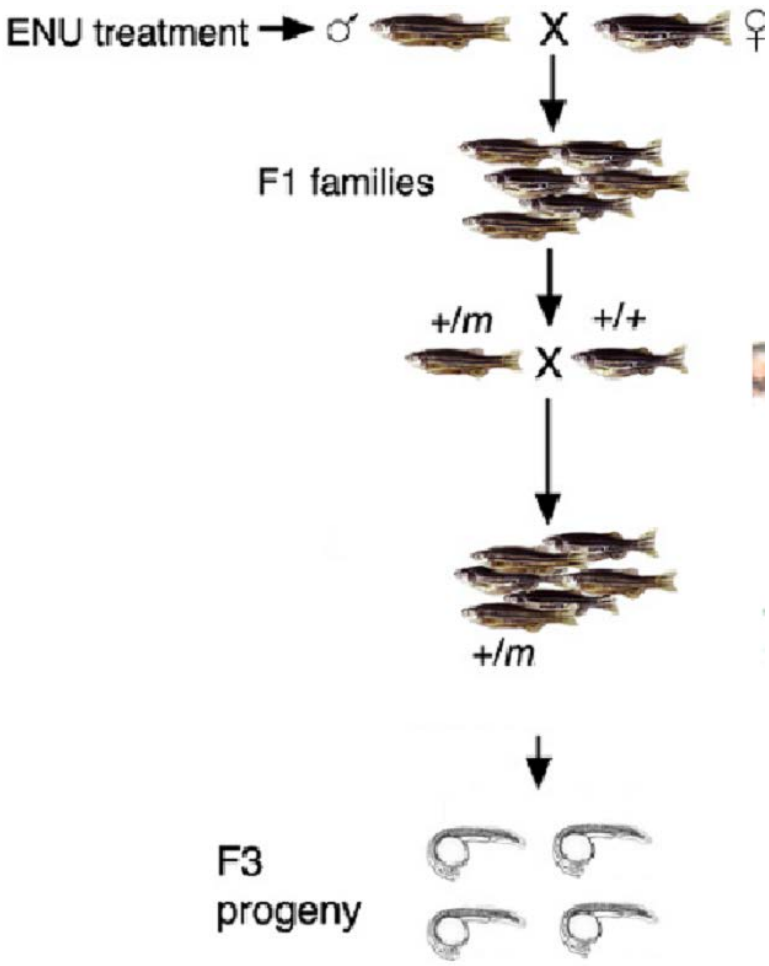

Figure 1.2 Mating scheme for forward screen and identification of phenotypes. Mutagenized males were outcrossed with wildtypes (Tu strain) to obtain F1 and F2 generations. The F2s were in-crossed and screened for lack of adipose tissue mass.

1.2.2 Breeding strategy for map cross

We identified the heterozygous fish from the F2 family that inherited the phenotype (lack of adipose tissue) in an autosomal recessive pattern (3:1). For positional cloning, we outcrossed these F2 to wildtype AB strain. We further screened and identified the heterozygous carrier pair that consistently inherited the mutation in autosomal recessive pattern. We used the progeny from these heterozygous pairs for genetic mapping and positional cloning.

1.2.3 Nile red staining

The Nile red (NR) staining was performed on live 18 dpf larvae. A 500 µg/ml stock NR solution was prepared in acetone. Just before use, the working solution was obtained by 1/100 dilution of stock in fish water. Live larvae were then exposed to a NR working solution in the dark for 30 min at 28 ^{o}C till the NR adipocyte stain saturated. The larvae were then rinsed twice with fish water for 5 minutes, anaesthetized in 0.4% tricaine (w/v) pH 7.1, and observed under a fluorescence microscope (29).

1.2.4 Extraction of DNA from zebrafish larvae

The 18-dpf larvae were treatment with cell lysis buffer (10 mM Tris-HCL), [pH 8.0], 10 mM NaCl, 0.5% NP-40, and Proteinase K) for 3 hours for complete digestion of the larvae. The lysate were centrifuged, and supernatant DNA was used for PCR analysis.

1.2.5 Analysis of 'z' markers

We ordered the primers sequences for selected 'z' markers that are available in the Ensembl database for zebrafish (http://uswest.ensembl.org/Danio_rerio). We amplified the genome DNA using these primers. The standard PCR was performed using the GoTaq Flexi DNA Polymerase kit (Promega). The PCR products were run on 4% agarose gel, and products from mutant pools, wildtype pools, and parents were compared.

1.2.6 Whole genome sequencing

Parent fish heterozygous for the *sns* mutation in the AB strain were in-crossed to generate the mutant larvae and wildtype siblings. The fixed and Oil red O (ORO) stained

18-dpf larvae scored for lack of lipid stains in adipose tissue. DNA was extracted from these larvae using DNeasy blood and tissue kit (Qiagen Cat. 69504). We pooled DNA from 43 larvae and processed for whole genome sequencing (WGS). Whole genomes from pooled DNA samples were sequenced by Illumina HiSeq2000 at the Huntsman Cancer Institute sequencing core, Utah. The process involved the fragmentation of genomic DNA into a library of small segments, PCR amplification, and high throughput sequencing.

1.2.7 Whole exome sequencing

We obtained DNA from larvae from the mutant larvae and WT sibling. For sorting, we bred the heterozygotes fish in AB strain, and the larvae were stained with NR staining. NR staining allowed live scoring of wildtype and mutant fish. Furthermore, it circumvented paraformaldehyde treatment, which fragments the genomic DNA and lowers the genomic DNA yield. We pooled the DNA from the 13 mutant larvae and sent for Hi-Seq2000 Illumina sequencing to the commercial vendor Optogenetics. In parallel, we also sequenced pooled DNA from 15 WT siblings. Whole exome sequencing (WES) is a method that allows a rapid identification of protein coding mutation including missense, nonsense, splice site, and small deletion/insertion mutations. The process involved enrichment of exons from genomic DNA followed by high throughput sequencing of the exon-enriched samples.

1.2.8 Sanger sequencing of candidate SNPs

We amplified the genome DNA using the primers that amplified the genomic region of DNA that flanks the candidate regions. The primers were designed using an Ape-A plasmid editor. The primers used for amplifying candidate variant on Chr1 (ENSDARG00000052899) were forward 5'-gacaaatcaagagcacacacact-3' and reverse 5'-ctggcgtttcccatgttctt-3'. The primers used for amplifying candidate variant on Chr5 (ENSDARG00000004392) were forward 5'-cttcataataccctcacctctaccct-3' and reverse 5'-ccagcagggcagtttagaca-3'. The primers used for amplifying candidate variant on Chr18 (ENSDARG00000040582) were forward 5'-aaagaagaggcccaagaaagacaat-3'and reverse 5'-ctggcgtttcccatgttctttga-3'. The primers used for amplifying candidate variant on Chr24 (ENSDARG00000062087) were forward 5'-gaggaggatggacagtcggaa-3' and reverse 5'-tgtcacttgtatttccctctcttgt -3'. The standard PCR was performed using GoTaq Flexi DNA Polymerase kit (Promega). Sanger sequencing was performed on the PCR purified amplicons.

1.3 Results

We mutagenized zebrafish and screened offspring for the absence of stainable lipids in adipose tissue to find gene(s) that affect lipid storage in adipose tissue. A conventional, recessive, third generation (F_3) mutagenesis screen was conducted. Male Tüebingen(Tü) fish were mutagenized with ethylnitrosourea (ENU). Members of individual F_2 families were incrossed, and their progeny were stained with ORO (24, 26). At 18-dpf, we stained and screened the zebrafish for reduced adipocyte lipid mass following a recessive inheritance pattern (Fig. 1.3). We have identified one mutant that follows this phenotypic pattern and have named it *sans suet* (*sns*).

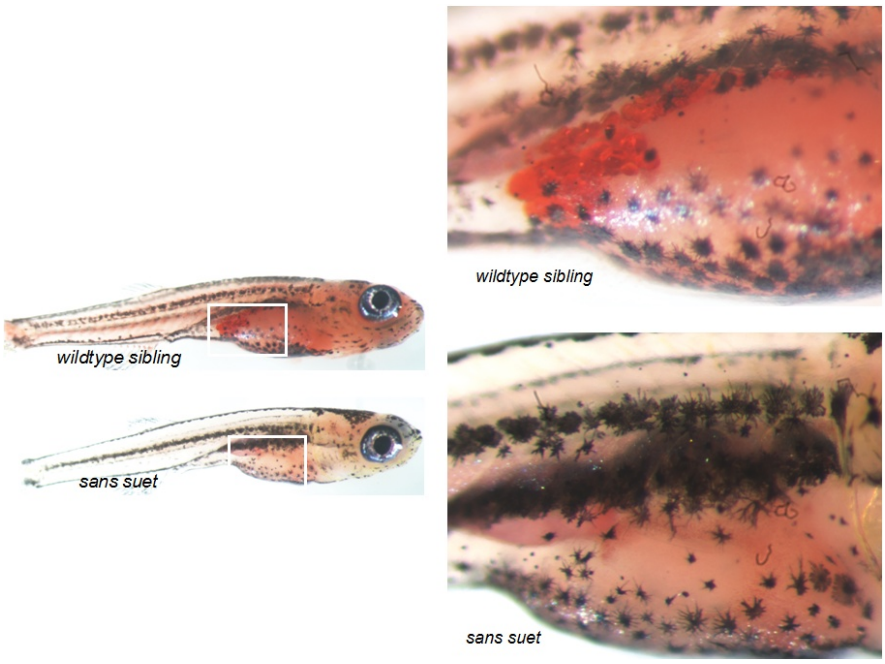

Figure 1.3 Oil Red O staining to visualize neutral lipid droplets at 18 dpf. (upper panel: wild type sibling and lower panel: *sans suet*)

1.3.1 Genetic mapping of *sns* mutation by SSLP markers

To identify the gene responsible for the *sns* mutation, our immediate goal was to map the *sns* mutation. To that end, our laboratory has employed traditional positional cloning techniques. Initially, our laboratory has used approximately 300 SSLP 'z' markers to find the genetic linkage (38), but we did not obtain linkage between the *sns* mutation and SSLP markers

1.3.2 Genetic mapping of *sns* mutation by WGS

The conventional mapping strategies utilize a predefined set of markers within pooled genome of mutants to derive the genomic regions that are linked with the mutant phenotype. Many markers are not polymorphic, in particular crosses or genetic background, and are therefore uninformative. The advent of next generation sequencing

(NGS) has increased the ability to map and identify mutation. In addition to mapping of the linkage region, NGS also provides sequence information within the linked interval. This enables the researcher to identify candidate mutations within the linked interval (38). We performed whole genome sequencing (WGS) on the *sns*$^{-/-}$ mutant larvae pool. We used a publicly available scheme (Galaxy Cloudmap) for variant discovery mapping (43). The analysis of WGS involved the alignment of sequenced short reads to reference genome (Zv9) using the Burrow-Wheeler aligner (BWA) (44). This program allowed the researcher to efficiently align short sequence reads against a larger reference sequence, allowing identification of mismatches and gaps. The identification of variants was performed using the genome analysis toolkit (GATK) (45). We hypothesize that genomic regions that are linked to the causal mutation will have low recombination. Thus, the region will have a stretch of pure parental sequences and be devoid of mapping strain sequences (43).

Based on the scatter plot we obtained from variant discovery mapping, we predicted the linkage group as shown in Fig. 1.4. To validate that true linkage group versus chance, we selected the 'z' markers that covered these genomic regions. We determined the SSLP on wildtype pool, mutant pool, and heterozygous parents. We screened SSLP markers (z4273, z4188, z1146, z8450) that covered 25Mb to 35Mb of chromosome 12. Similarly, we screened SSLP markers (z9488, z40230, z9189, z40745, z7070, G40006, G41815) that covered from 27 to 35 Mb of chromosome 15 and (z22659, z8809, z21170, z8976, z7158, z10758, z21401, z4304) that covered 20 to 31 MB of chromosome 20. The PCR and electrophoresis from SSLP markers showed no linkage in these regions.

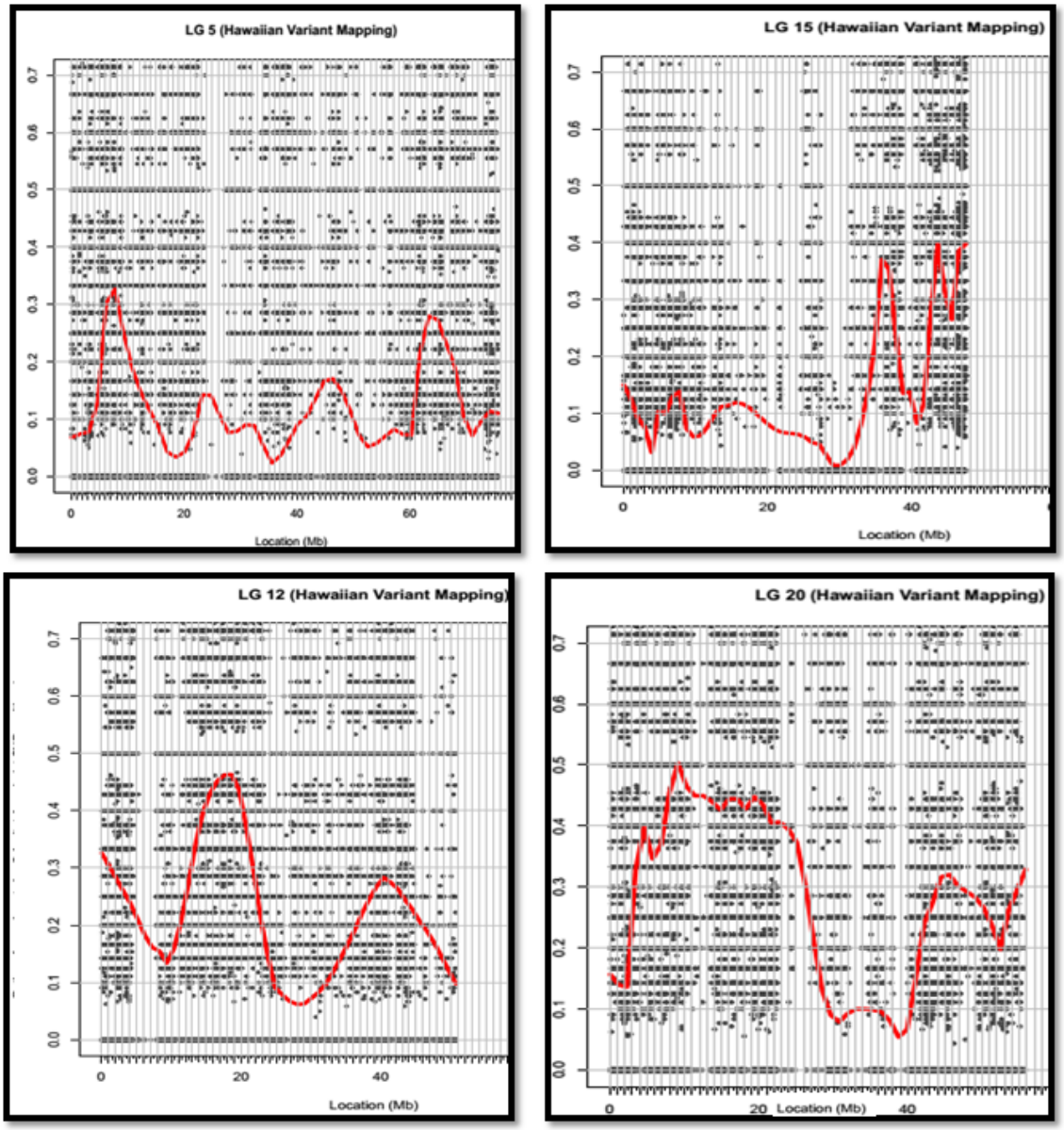

Figure 1.4 Galaxy Cloudmap scatter plot. The scatter plot represents the ratio of the number of reads of reference strain to the number of reads of (mutant) parental strain plotted against the chromosomal region (Mb). The linear regression line represents the trend of variants on the genome. The linkage group (LG) number represents the chromosome number.

1.3.3 Genetic mapping of *sns* mutation by WES

WES is now used to isolate mutations in humans and other model system (46, 47). Recently, the WES based methodology is described for the mapping and rapid isolation of mutations recovered from forward genetics (48). WES technology for mapping has proved robust with identification of missense, nonsense, and splice-site mutations. Exon enrichment, high coverage sequencing technology, and publicly available analysis software made WES a feasible alternative for mapping and identification of mutations in zebrafish. The SNP variant in zebrafish is not completely characterized compared to other model organisms. The sequencing of the pool of unaffected larvae is required to identify the complete spectrum of informative variant in zebrafish (38). Thus, we utilized robust WES to sequence whole exomes from pools of *sns*$^{-/-}$ mutants and WT siblings.

Analysis of NGS data with SNP track has been previously used to find the linkage and candidate mutation (38). We applied a similar approach to analyze WES in our mutant pool and WT sibling pools. We did not obtain the peak at single chromosomal region suggestive of linkage as anticipated. In contrast, we found multiple peaks at various chromosomal regions (Fig. 1.5). Since SSLP markers were not informative in previous attempts to establish the linkage, we attempted to establish the genetic linkage using variants that are obtained in both WGS and WES. To further investigate variant and determine candidate linkage region, we established the following criteria: a) variant must be homozygous in both WES and WGS, b) variant must have depth of coverage of at least 5 in whole genome sequence data and whole exome sequencing, c) variant must have human ortholog, and d) variant must induce a nonsynonymous mutation. Based on these criteria, we obtained four different candidate mutations in different genomic

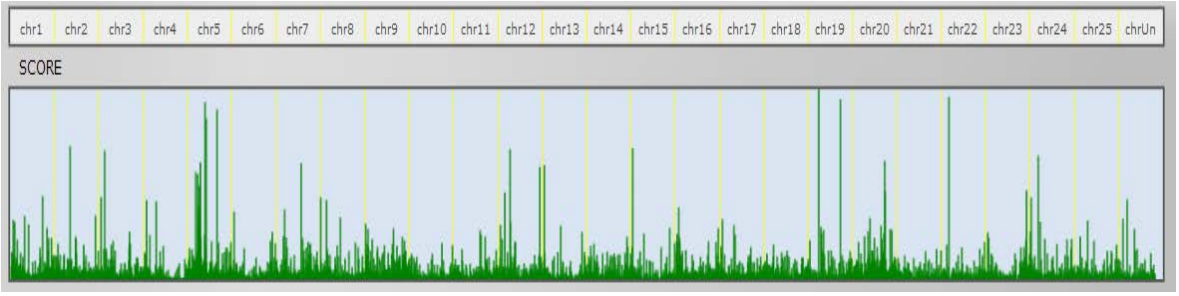

Figure 1.5 Graph represents for variants in WES. The peaks represent arbitrary score for variants in the mutant pool compared against WT sibling pools. The peak density and height represent variant in these chromosomal regions.

regions. The candidates region obtained are shown in Table 1.1.

1.3.4 Targeted sequencing of candidate variants

We designed the primer that amplifies the region and variant position mentioned in Table 1.1. We performed Sanger sequencing of these four different SNPs to determine if any of these regions are linked. We hypothesized that the linked region should be homozygous in mutant pool but heterozygous in WT pool. The candidate SNPs on Chr1, Chr18, and Chr24 were homozygous background mutations that were found in both mutant pool and wildtype pool. The variant in *hdr* gene in Chr5 was heterozygous (G&A) in mutant pool (Fig. 1.6).

1.4 Discussion

Lipid storage in adipose tissues is affected by multiple factors. The characterization of *sns* mutant is crucial to understanding the phenotype. We hypothesize different scenarios that can result in a lack of stainable lipids in adipose tissue. First, the *sns* mutation may be linked to lipodystrophy where WAT lipid storage is altered due to decreased lipid uptake, synthesis, or droplet formation. This results in metabolic complications such as hepatic steatosis, hypertryglyceridemia, and insulin resistance (23). Second, the *sns* mutation may be linked to processes such as fatty acid synthesis, desaturation, or elongation or fatty acid oxidation. A defect in these processes result in decreased lipogenesis, decreased lipid storage, increased fatty acid oxidation, and resistant to diet induced insulin resistance (15–17). Third, the *sns* mutation may be associated with defect in adipose tissue development, tissue patterning, or survival

Table 1.1 The candidate genomic region (from ensembl) based on the above criteria.

Chr	Position	Gene symbol	Gene Name	Human Orthologue	Base change
1	41134904	ENSDARG00000052899	Uncharacterized	ENSG00000133574	GAC/GTC
5	29051561	ENSDARG00000004392	Hdr	ENSG00000104689	GGG/AGG
18	32379671	ENSDARG00000040582	C18H3orf33	ENSG00000174928	CGG/TGG
24	27766771	ENSDARG00000062087	nceh1b	ENSG00000144959	CTT/TTT

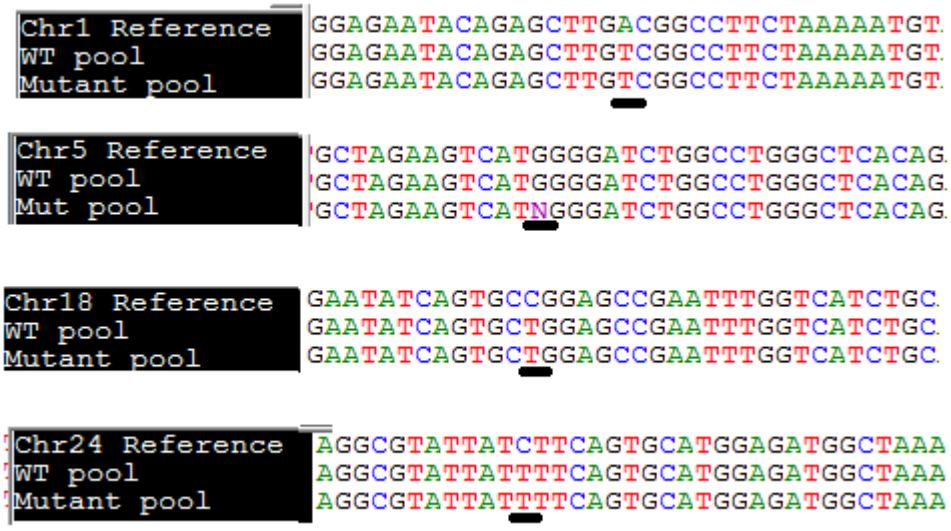

Figure 1.6 Alignment of PCR sequences of WT sibling pool and Mutant pool of *sns* mutant.

(31, 49, 50). Finally, the *sns* mutation may be associated with defect in uptake of lipids in intestine or altered feeding behavior (18–22). The characterization of mutant phenotype could shed light on processes responsible for the phenotype.

We have used SSLP markers and next generation sequence analysis to determine the linkage of *sns* mutation. We have performed targeted SSLP marker analysis and SNP analysis in the regions that are derived from NGS approaches. We observed that variant at the *hdr* gene at chromosome 5 is heterozygous in mutant pool. The whole genome sequencing (Fig. 1.4) and whole exome sequencing analysis (Fig. 1.5) suggested that the region near 30 Mb of Chr5 regions have differences in the variant distribution compared to reference genome and WT sibling. Although the variant on the *hdr* gene is heterozygous, the region near these may have a stretch of a homozygous region that is suggestive of linkage. We only tested the nonsynonymous coding locus, but the variant may lie in the regulatory regions that were not considered during analysis. The *sns* mutation could be due to copy number variants. The bioinformatic software, such as EXCAVATOR, has been devised to detect the copy number variant from whole exome sequencing data (51).

Zebrafish are not a completely inbred model, and some background SNPs haplotypes are shared between different strains. The chemical mutagenesis was performed on Tu strain that have high structural background variants (52). These background mutations may have hindered the genetic mapping with both SSLP markers and NGS approaches. In these cases, diluting the Tu strain by breeding the heterozygous *sns* mutant pair to other WT strains may provide informative polymorphic markers and successful genetic mapping. We have bred heterozygous *sns* parents with wildtype AB strain. Identified

heterozygous pairs and progeny from this outcross should be used for future mapping. Furthermore, prescreening and selection of informative polymorphic markers in mapping and mutant background strain could increase the linkage mapping efficiency. The next generation sequencing technology may be utilized for rapid and robust genetic mapping.

Other possibilities may be regions that are not completely covered during high throughput sequencing or low quality assembly of reference genome. In these cases, visualizing alignment of sequence in that particular region, Sanger sequencing on the low coverage region and virtual chromosome walking with BACs should be employed (53). The sequencing reads may be misaligned and duplicated during genome sequence analysis. In a previous study, the bioinformatic approach to remove the duplicated assembly of the reference genome has been shown to improve the linkage mapping (38). Alternately, linkage mapping is hindered when the phenotypic overlap between wildtype and mutant results in erroneous scoring of wildtype as a mutant. To determine true homozygous mutants, the mutant pools are being bred to examine the phenotypic ratio in progeny. The mutants that have the expected Mendelian phenotype ratio may be used for future cloning and characterization of *sns* mutation.

CHAPTER 2

DEVELOP TRANSGENIC TOOLS TO STUDY ADIPOGENESIS

2.1 Introduction

Previous studies have elegantly determined that adipose tissues are composed of precursor cells, adipocytes, and other cell types (6). It has now been revealed that new adipocytes are formed constantly to maintain the adipose tissue in human adults (54). The acute exposure to calorie excess results in increased adipocyte size. In contrast, the chronic high fat diet results in increased adipose size and number. It has been hypothesized that the adipocytes undergo hypertrophy to a threshold. After that, the precursor cells are recruited and committed to form new adipocytes (54, 55). The molecular basis for this regulation of adipose tissue dynamics is not fully understood. It is debatable whether the new adipose tissue is formed to compensate the metabolic demands in calorie excess. Thus, understanding adipogenesis in various nutritional states is vital to appreciate its importance. Our goal is to develop molecular tools in zebrafish to study adipogenesis. The study of adipose biology in zebrafish suffers from a lack of tools to visualize and genetically manipulate adipocytes. We aimed to develop a transgenic reporter line that specifically labels adipocytes in zebrafish. Fluorescently labeling adipose tissue enables us to survey the adipose tissues dynamics in response to various

nutrients in both larval and adult stages. With the transgenic reporter tools, we can interrogate how adipogenesis is influenced by genetic, nutritional, and chemical factors. The transgenic reporter fish will allow us to monitor cell size and cell number *in vivo* fluorescence imaging. A previous study has shown that zebrafish are amenable for exploring chemical modulators of adipose tissue metabolism (29). In the long term, we will also a use a transgenic reporter to perform large genetic and chemical screens to find novel genes and pathways that modulate adipose tissue metabolism. Utilizing these tools, we may advance our understanding of adipose tissues and related disorders that may impact future therapeutic approaches and potential therapy.

2.1.1 Meganucleases and transposases mediated transgenesis

Over the past decade, Isce-I meganuclease and Tol2 transposase mediated transgenesis has been developed to allow efficient integration into a host genome and transmission to successive generations. These technologies have been used to drive a whole body or tissue specific expression of reporters, genes that have allowed dissection of gene function at the molecular level and in a tissue specific manner (56, 57). Utilizing these two technologies, various groups have successfully integrated a bacterial artificial chromosome (BAC) as well as a short functional promoter fraction to create transgenic reporters. BACs encompass approximately 350 kb fragments including regulatory sequences and can be re-engineered and modified to contain reporters of choice to create stable transgenic animals (57, 58). There are daunting technical challenges in dealing with large BAC engineering and genomic integration. To circumvent these potential difficulties, the short functional promoter fragments are used to design and create tissue

specific reporter and transgenic tools. Placing these functional promoters at the 5' end of a reporter cassette fully recapitulates the endogenous expression pattern. The caveat is identification of a minimal promoter fragment that encompasses the essential regulatory elements to mimic endogenous expression (59). Despite numerous efforts, we and others have been unable to identify a short functional promoter that drives tissue specific expression in adipocytes. Our laboratory has tried 5' upstream DNA fragment of *adipoq*, *plin2*, and the full mouse *ap2* promoter to drive expression of transgenes without success.

2.1.2 TALEN based genome engineering tools

Genome engineering is the modification of the genome at a precise and predefined locus. In recent years, the emergence of novel genome engineering tools such as zinc finger nuclease (ZFN), Trascriptional Activator Like Effector Nuclease (TALEN), and clustered regularly interspaced short palindromic repeats (CRISPR) has allowed efficient and effective transgenesis in an unprecedented manner. Studies have reported that gene targeting through homologous recombination events are enhanced by several orders of magnitude using nucleases (ZFN, TALEN) (60). The double strand break created by these nucleases are efficiently repaired by error prone nonhomologous end joining (NHEJ), resulting in gene disruption. In the presence of homologous donor DNA NHEJ, and homology directed repair (HDR) result in integration of donor DNA into the host genome, resulting in targeted gene modification (61).

TALEN is a genome engineering nuclease created by fusion of a Transcription Activator Like Effector (TALE) and the type II FokI restriction enzyme (60). TALE is a plant pathogen protein that has specific and selective binding to DNA. The DNA

recognition elements are a series of tandem repeats (34 amino acids for TALEs). The TALE repeat recognizes a single base pair of DNA. The repeats are highly conserved except for two amino acids at positions 12 and 13. These variable diresidues (RVDs) appear to specify the base pairing (62, 63). The DNA binding motif can be modified and designed to bind the target DNA of interest. Asn-Asn, Asn-Ile, His-Asp, and Asn-Gly are four different RVD modules that recognized guanine, adenine, cytosine, and thymine, respectively (60). Upon binding two TALENs to predefined sites of DNA, formation of the FokI subdomain dimer cleaves the target DNA in the genome (Fig. 2.1). The TALEN exhibits significantly reduced off-target effects and cytotoxicities (64). TALENs have been used to create null mutations and conditional alleles in zebrafish, *Drosophila*, and mice (64–66).

TALEN has proven efficient to introduce locus-specific DNA replacement in both somatic and germline tissues (60). Recently, studies have shown that both single-stranded oligonucleotides and double-stranded eGFP cassettes can be inserted into a predefined region in the zebrafish genome through HDR, but the precise HDR was less frequent than error prone NHEJ-mediated integration. In these studies, donor DNA was flanked by the homologous arm to guide proper integration of donor DNA into the zebrafish genome (67).

We are employing TALEN-based genome engineering technology to create transgenic zebrafish that express mCherry-CAAX exclusively in adipocyte. Because of the adipocyte-specific expression of *fabp11a,* we aimed to construct a reporter that drives the expression of mCherry-CAAX under the endogenous *fabp11a* promoter. We are targeting the 3'end of *fabp11a* gene with the hypothesis that our approach expresses both

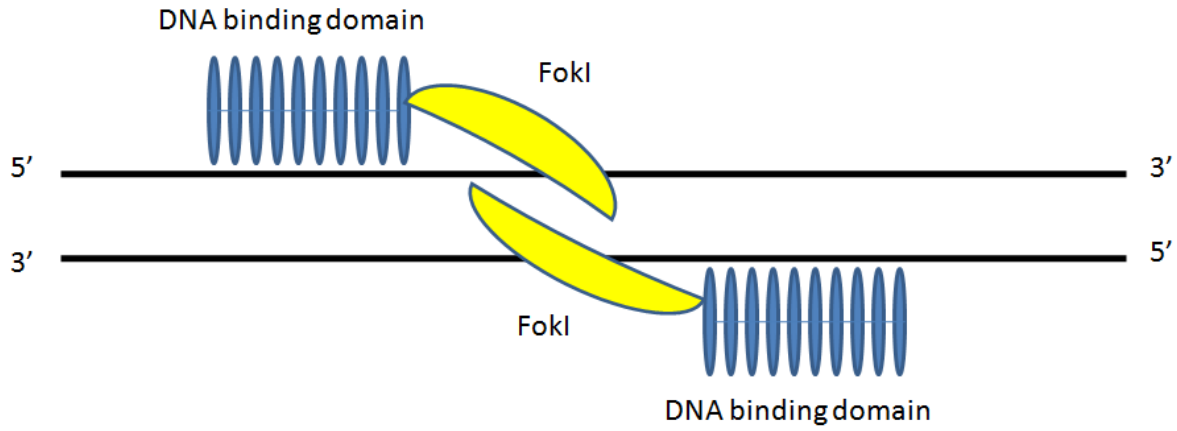

Figure 2.1 Representation of the TALEN binding to target DNA. The 34 amino acid tandem repeats bind to target DNA resulting in dimerization of FokI endonuclease. The dimerization of FokI introduces the double strand break in the spacer region of the target DNA.

fabp11a gene and *mCherry-CAAX* in a bicistronic manner. The principle and strategy is outlined in Fig. 2.1

2.2 Materials and Methods

2.2.1 TALEN design and assembly

The TALEN was designed by the Mutation Generation and Analysis Core, University of Utah. For designing TALEN, the exon 4 sequence of the *fabp11a* gene was screened for potential target sites using a TALEN targeter program (https://tale-nt.cac.cornell.edu/node/add/talen). The pCS2-*fab11a*-TALENL and pCS2 *fabp11a*-TALENR pair of TALEN plasmid was cloned using the Golden Gate Assembly system.

2.2.2 Designing the reporter construct

The reporter construct sequences were designed as shown in Fig. 2.2. We obtained the mCherry-CAAX construct flanked by the homologous arm from gene synthesis, Genewiz, NJ.

2.2.3 Synthesis of TALEN mRNA and injections

For *in vitro* mRNA synthesis, the TALEN plasmids were linearized using NotI restriction enzymes. The *in vitro* TALEN 5'capped mRNA was synthesized by using the mMessage mMachine SP6 kit. For *in vitro* transcription, 10 uL of 2X NTP/CAP, 2 ul of 10X Reaction buffer, 1 ug of linearized plasmid, and 2 uM of enzyme mix was added and incubated for 2 hours. After 2 hours, 1uL of Turbo DNase was added to hydrolyze linearized plasmid. mRNA was purified using RNeasy Qiagen kit. About 100 embryos incubated for 2 hours. After 2 hours, 1uL of Turbo DNase was added to hydrolyze linearized plasmid. mRNA was purified using RNeasy Qiagen kit. About 100 embryos were co-injected with TALEN mRNA and 100 pg of mCherry construct. We have injected 100, 200, and 500 pg of TALEN mRNA to determine the optimal cleavage activity of TALEN.

2.2.4 High resolution melting analysis

The TALEN induced mutation was detected using high resolution melting analysis as previously described (67). The PCR amplification of the target sites were performed using primers (forward 5'-ttgacaccaaagcaaatgctcact-3', reverse 5'-gcagggatcaacaaagcacaact-3') that flanked two TALEN binding sites. The amplified DNA

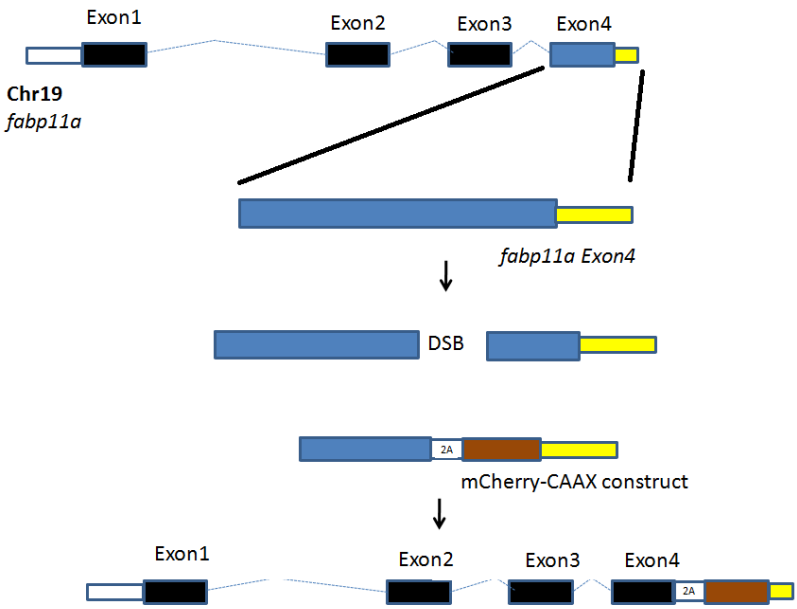

Figure 2.2 Principle and strategy for integration of mCherry-CAAX into the genome. Stepwise cleavage of genome and integration of mCherry construct into the genome. The TALEN L and TALEN R bind to the target site, form a FokI dimer, and cleave the spacer region, creating a double strand break (DSB). The mCherry-CAAX construct will be integrated by homology-directed recombination (HDR).

product was scanned by light scanner (Idaho technology) to determine the melting curve.

2.3 Results

2.3.1 *fabp11a* TALEN sites design and assembly

FABP belongs to the family of intracellular lipid binding proteins (iLBP) that bind to fatty acids in the cells (68). The mammalian *Fapb4* (also called adipocyte protein 2 -ap2) is a member of the iLBP family that is highly expressed in adipocytes and is considered a marker of differentiated adipocytes. The *Fabp4* gene is also expressed in macrophages and dendritic cells (69). Zebrafish have two homologues of mammalian *Fabp4,* i.e., *fabp11a* and *fabp11b* (70). It is observed that the *fabp11a* gene is highly expressed in

mature adipocytes (27) and functions in lipid binding and transport. The *Fabp4* promoter sequence is widely used for adipose tissue specific expression of the transgene in mice. Considering these facts, we choose *fabp11a* as a candidate for inserting the mCherry gene cassette at the 3' end of the gene. We designed the TALEN binds target DNA site near the 3' boundary regions of exon 4 as shown in Fig. 2.3a.

2.3.2 mCherry-CAAX constructs design and assembly

We designed a reporter construct that consists of a cDNA that encodes the membrane-bound mCherry-CAAX as shown in (Fig. 2.3b). Addition of the CAAX prenylation signal at the C-terminus of mCherry tethers mCherry to the plasma membrane (71). The membrane localization of the reporter has been shown to enhance the signal in adipocytes (49). Immediately upstream of the mCherry sequence, we placed the viral 2A peptide coding sequence. When a ribosome encounters a 2A sequence, peptide bond formation between a particular glycine and proline fails, resulting in 2 peptides (72). This permits the expression of the mCherry-CAAX reporter under the endogenous *fabp11a* promoter without disrupting endogenous *fabp11a* gene expression and fabp11a protein function. The flanking homologous arms direct integration of the construct during HDR / NHEJ DNA repair of the double-strand break introduced by the *fabp11a* TALEN **(**Fig. 2.2) (64, 65). The integration of the double stranded construct depends on the identity of the homologous arm to the target site and the length of the homologous arm (67).

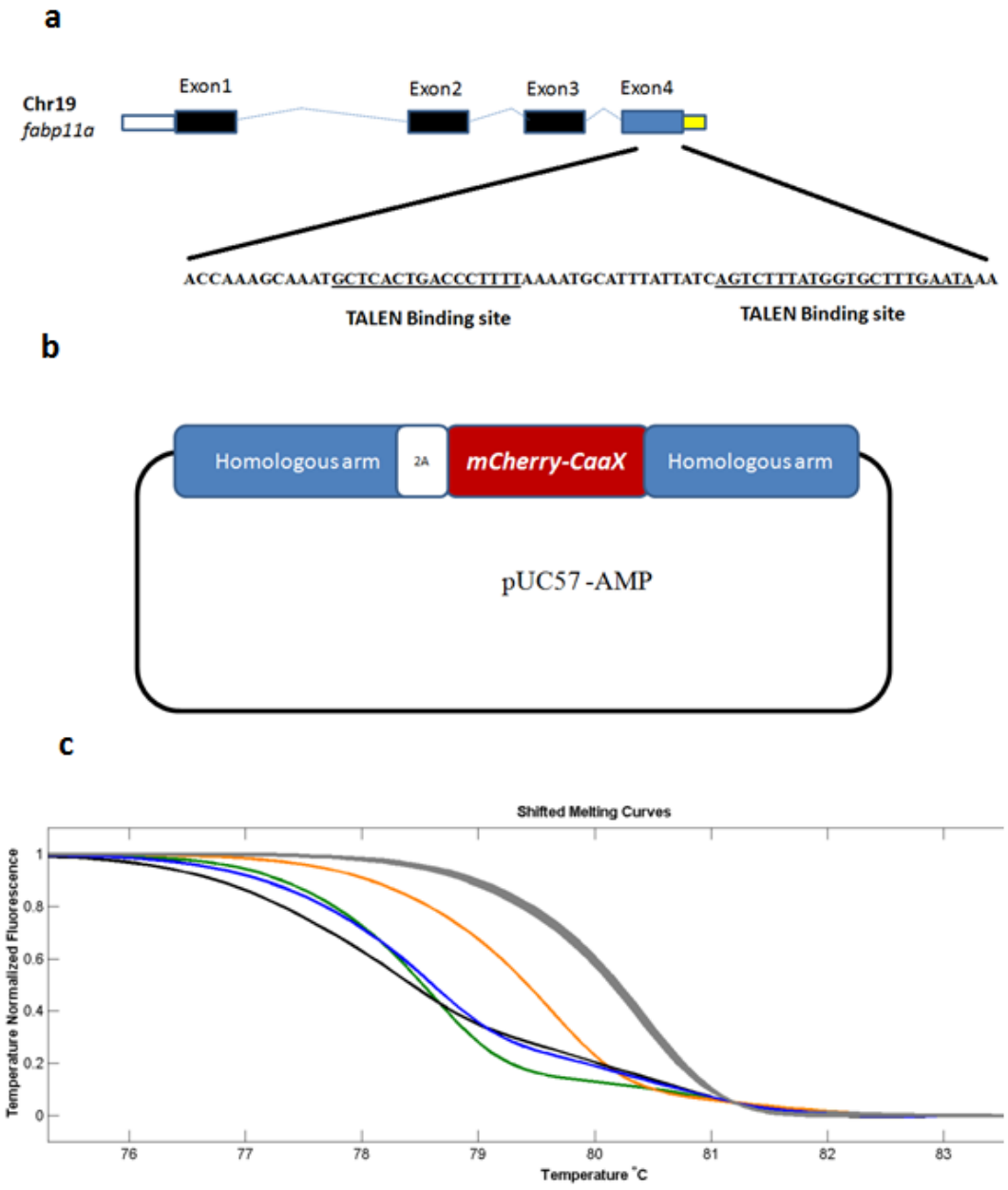

Figure 2.3 Representation of the TALEN binding site, mCherry construct assembly, and TALEN activity. a) Representation of the TALEN binding site on exon 4 of the fabp11a gene**. b)** Represents donor plasmid mCherry-CAAX flanked by homologous arms. c) HRMA analysis of fabp11a TALEN mRNA (400 pg) injected embryos. 4/50 injected zebrafish showed the shift (to the left) in the melting curve, which shows low efficiency of TALENs.

2.3.3 Determination of TALEN activity

We injected 100 pg, 200 pg, and 400 pg of TALEN mRNA into one-cell stage zebrafish embryos (Fig. 2.3c). If the TALEN creates the double-strand break in the predefined region of fabp11a gene, the host recruits and activates the error prone NHEJ repair machinery, resulting in mutation in the genome. The induced mutation can be analyzed using HRMA. The result suggests that the TALEN activity introducing the double strand break in the genome of zebrafish was low even at high concentration (400pg) of TALEN RNA. Most studies have found that the 100 to 200 pg of TALEN is sufficient to efficiently create a double-strand break in the genome.

2.4 Discussion

In principle, the TALEN DNA binding domain can be manipulated to introduce a double-strand break at any target site. There are multiple factors that may influence its binding and nuclease activity. The TALEN activity depends on the target site complexity, amount of TALEN mRNA injected, TALEN binding, and injection to embryos (64). Alteration in a single base can reduce the TALEN binding to the target site in the genome. We have used genotyped animals that have no mutation at the TALEN binding site. Previous studies have revealed that introduction of a double strand break depends on the amount of the TALEN mRNA injected into embryos. The literature has reported that approximately 100 to 200 pg of TALEN mRNA is needed for an efficient double strand break (64, 65). We have increased the concentration to 400 pg of TALEN mRNA. We have not obtained an efficient DSB in the target site. So far, there are no tools to predict the activity of TALEN before experimental validation, but *in vitro* binding and cleavage

assay have been previously used to determine the DNA binding and nuclease activity of TALEN (73). This assay will help us to determine if the *fabp11a* TALEN we have designed is able to bind the target site and introduce a double strand break. This involves the synthesis of a short stretch of target DNA and assay with TALEN protein to determine the cleavage of the target DNA *in vitro*.

The target complexity is the inherent issue associated with TALEN activity *in vivo*. The chromatin state and DNA methylation site hinder the binding of TALEN to the target DNA (60). Complete evidence on DNA methylation and the chromatin state of *fabp11a* gene during the embryonic stage is not available. The CRISPR/Cas9 system is alternate genome engineering tools that can be utilized to introduce DSB in target site. CRISPR/Cas9 system is not sensitive to the methylation state of the genome region compared to TALENs (67). Since it is an RNA guided nuclease system, it is simpler to design compared to TALENs and ZFNs (60).

REFERENCES

1. Tauchi-Sato, K., Ozeki, S., Houjou, T., Taguchi, R., and Fujimoto, T. (2002) The surface of lipid droplets is a phospholipid monolayer with a unique Fatty Acid composition. *J. Biol. Chem.* **277**, 44507–44512

2. Schlegel, A., and Stainier, D. Y. (2007) Lessons from "lower" organisms: what worms, flies, and zebrafish can teach us about human energy metabolism. *PLoS Genet.* **3**, e199

3. Lowe, C. E., O'Rahilly, S., and Rochford, J. J. (2011) Adipogenesis at a glance. *J. Cell Sci.* **124**, 2681–2686

4. Rosen, E. D., and Spiegelman, B. M. (2014) What we talk about when we talk about fat. *Cell* **156**, 20–44

5. Tang, Q. Q., and Lane, M. D. (2012) Adipogenesis: from stem cell to adipocyte. *Annu. Rev. Biochem.* **81**, 715–736

6. Berry, D. C., Stenesen, D., Zeve, D., and Graff, J. M. (2013) The developmental origins of adipose tissue. *Development* **140**, 3939–3949

7. Rosen, E. D., Walkey, C. J., Puigserver, P., and Spiegelman, B. M. (2000) Transcriptional regulation of adipogenesis. *Genes Dev.* **14**, 1293–1307

8. Cristancho, A. G., and Lazar, M. A. (2011) Forming functional fat: a growing understanding of adipocyte differentiation. *Nat. Rev. Mol. Cell. Biol.* **12**, 722–734

9. Sethi, J. K., and Vidal-Puig, A. J. (2007) Thematic review series: adipocyte biology. Adipose tissue function and plasticity orchestrate nutritional adaptation. *J. Lipid Res.* **48**, 1253–1262

10. Ashrafi, K., Chang, F. Y., Watts, J. L., Fraser, A. G., Kamath, R. S., Ahringer, J., and Ruvkun, G. (2003) Genome-wide RNAi analysis of Caenorhabditis elegans fat regulatory genes. *Nature* **421**, 268–272

11. Szymanski, K. M., Binns, D., Bartz, R., Grishin, N. V., Li, W. P., Agarwal, A. K., Garg, A., Anderson, R. G., and Goodman, J. M. (2007) The lipodystrophy protein seipin is found at endoplasmic reticulum lipid droplet junctions and is important for droplet morphology. *Proc. Natl. Acad. Sci. U. S. A.* **104**, 20890–20895

12. Pospisilik, J. A., Schramek, D., Schnidar, H., Cronin, S. J., Nehme, N. T., Zhang, X., Knauf, C., Cani, P. D., Aumayr, K., Todoric, J., Bayer, M., Haschemi, A., Puviindran, V., Tar, K., Orthofer, M., Neely, G. G., Dietzl, G., Manoukian, A., Funovics, M., Prager, G., Wagner, O., Ferrandon, D., Aberger, F., Hui, C. C., Esterbauer, H., and Penninger, J. M. (2010) Drosophila genome-wide obesity screen reveals hedgehog as a determinant of brown versus white adipose cell fate. *Cell* **140**, 148–160

13. Sohle, J., Machuy, N., Smailbegovic, E., Holtzmann, U., Gronniger, E., Wenck, H., Stab, F., and Winnefeld, M. (2012) Identification of new genes involved in human adipogenesis and fat storage. *PLoS One* **7**, e31193

14. Baumbach, J., Hummel, P., Bickmeyer, I., Kowalczyk, K. M., Frank, M., Knorr, K., Hildebrandt, A., Riedel, D., Jackle, H., and Kuhnlein, R. P. (2014) A Drosophila in vivo screen identifies store-operated calcium entry as a key regulator of adiposity. *Cell Metab.* **19**, 331–343

15. Abu-Elheiga, L., Matzuk, M. M., Abo-Hashema, K. A., and Wakil, S. J. (2001) Continuous fatty acid oxidation and reduced fat storage in mice lacking acetyl-CoA carboxylase 2. *Science* **291**, 2613–2616

16. Zadravec, D., Brolinson, A., Fisher, R. M., Carneheim, C., Csikasz, R. I., Bertrand-Michel, J., Boren, J., Guillou, H., Rudling, M., and Jacobsson, A. (2010) Ablation of the very-long-chain fatty acid elongase ELOVL3 in mice leads to constrained lipid storage and resistance to diet-induced obesity. *FASEB J.* **24**, 4366–4377

17. Shi, X., Li, J., Zou, X., Greggain, J., Rodkaer, S. V., Faergeman, N. J., Liang, B., and Watts, J. L. (2013) Regulation of lipid droplet size and phospholipid composition by stearoyl-CoA desaturase. *J. Lipid. Res.* **54**, 2504–2514

18. Ho, S. Y., Lorent, K., Pack, M., and Farber, S. A. (2006) Zebrafish fat-free is required for intestinal lipid absorption and Golgi apparatus structure. *Cell Metab.* **3**, 289–300

19. Schwartz, M. W., Woods, S. C., Porte, D., Jr., Seeley, R. J., and Baskin, D. G. (2000) Central nervous system control of food intake. *Nature* **404**, 661–671

20. Cohen, P., Zhao, C., Cai, X., Montez, J. M., Rohani, S. C., Feinstein, P., Mombaerts, P., and Friedman, J. M. (2001) Selective deletion of leptin receptor in neurons leads to obesity. *J. Clin. Invest.* **108**, 1113–1121

21. Zhang, W., Cline, M. A., and Gilbert, E. R. (2014) Hypothalamus-adipose tissue crosstalk: neuropeptide Y and the regulation of energy metabolism. *Nutr Metab (Lond)* **11**, 27

22. Smemo, S., Tena, J. J., Kim, K. H., Gamazon, E. R., Sakabe, N. J., Gomez-Marin, C., Aneas, I., Credidio, F. L., Sobreira, D. R., Wasserman, N. F., Lee, J. H.,

Puviindran, V., Tam, D., Shen, M., Son, J. E., Vakili, N. A., Sung, H. K., Naranjo, S., Acemel, R. D., Manzanares, M., Nagy, A., Cox, N. J., Hui, C. C., Gomez-Skarmeta, J. L., and Nobrega, M. A. (2014) Obesity-associated variants within FTO form long-range functional connections with IRX3. *Nature* **507**, 371–375

23. Garg, A., and Agarwal, A. K. (2009) Lipodystrophies: disorders of adipose tissue biology. *Biochim. Biophys. Acta* **1791**, 507–513

24. Patton, E. E., and Zon, L. I. (2001) The art and design of genetic screens: zebrafish. *Nat. Rev. Genet.* **2**, 956–966

25. Lawson, N. D., and Wolfe, S. A. (2011) Forward and reverse genetic approaches for the analysis of vertebrate development in the zebrafish. *Dev. Cell* **21**, 48–64

26. Schlegel, A. (2012) Studying non-alcoholic fatty liver disease with zebrafish: a confluence of optics, genetics, and physiology. *Cell. Mol. Life Sci.* **10,** 132-146

27. Flynn, E. J., 3rd, Trent, C. M., and Rawls, J. F. (2009) Ontogeny and nutritional control of adipogenesis in zebrafish (Danio rerio). *J. Lipid Res.* **50**, 1641–1652

28. Imrie, D., and Sadler, K. C. (2010) White adipose tissue development in zebrafish is regulated by both developmental time and fish size. *Dev. Dyn.* **239**, 3013–3023

29. Tingaud-Sequeira, A., Ouadah, N., and Babin, P. J. (2011) Zebrafish obesogenic test: a tool for screening molecules that target adiposity. *J. Lipid Res.* **52**, 1765–1772

30. Chang, J., Wang, M., Gui, W., Zhao, Y., Yu, L., and Zhu, G. (2012) Changes in thyroid hormone levels during zebrafish development. *Zoolog. Sci.* **29**, 181–184

31. Laudet, V. (2011) The origins and evolution of vertebrate metamorphosis. *Curr. Biol.* **21**, R726–737

32. Parichy, D. M., and Turner, J. M. (2003) Zebrafish puma mutant decouples pigment pattern and somatic metamorphosis. *Dev. Biol.* **256**, 242–257

33. Nelliot, A., Bond, N., and Hoshizaki, D. K. (2006) Fat-body remodeling in Drosophila melanogaster. *Genesis* **44**, 396–400

34. Zhou, Y., and Zon, L. I. (2011) The zon laboratory guide to positional cloning in zebrafish. *Methods Cell Biol.* **104**, 287–309

35. Obholzer, N., Swinburne, I. A., Schwab, E., Nechiporuk, A. V., Nicolson, T., and Megason, S. G. (2012) Rapid positional cloning of zebrafish mutations by linkage and homozygosity mapping using whole-genome sequencing. *Development* **139**, 4280–4290

36. Gupta, T., Marlow, F. L., Ferriola, D., Mackiewicz, K., Dapprich, J., Monos, D., and Mullins, M. C. (2010) Microtubule actin crosslinking factor 1 regulates the Balbiani body and animal-vegetal polarity of the zebrafish oocyte. *PLoS Genet.* **6**, e1001073

37. Bowen, M. E., Henke, K., Siegfried, K. R., Warman, M. L., and Harris, M. P. (2012) Efficient mapping and cloning of mutations in zebrafish by low-coverage whole-genome sequencing. *Genetics* **190**, 1017–1024

38. Leshchiner, I., Alexa, K., Kelsey, P., Adzhubei, I., Austin-Tse, C. A., Cooney, J. D., Anderson, H., King, M. J., Stottmann, R. W., Garnaas, M. K., Ha, S., Drummond, I. A., Paw, B. H., North, T. E., Beier, D. R., Goessling, W., and Sunyaev, S. R. (2012) Mutation mapping and identification by whole-genome sequencing. *Genome Res.* **22**, 1541–1548

39. Smith, D. R., Quinlan, A. R., Peckham, H. E., Makowsky, K., Tao, W., Woolf, B., Shen, L., Donahue, W. F., Tusneem, N., Stromberg, M. P., Stewart, D. A., Zhang, L., Ranade, S. S., Warner, J. B., Lee, C. C., Coleman, B. E., Zhang, Z., McLaughlin, S. F., Malek, J. A., Sorenson, J. M., Blanchard, A. P., Chapman, J., Hillman, D., Chen, F., Rokhsar, D. S., McKernan, K. J., Jeffries, T. W., Marth, G. T., and Richardson, P. M. (2008) Rapid whole-genome mutational profiling using next-generation sequencing technologies. *Genome Res.* **18**, 1638–1642

40. Austin, R. S., Vidaurre, D., Stamatiou, G., Breit, R., Provart, N. J., Bonetta, D., Zhang, J., Fung, P., Gong, Y., Wang, P. W., McCourt, P., and Guttman, D. S. (2011) Next-generation mapping of Arabidopsis genes. *Plant J.* **67**, 715–725

41. Blumenstiel, J. P., Noll, A. C., Griffiths, J. A., Perera, A. G., Walton, K. N., Gilliland, W. D., Hawley, R. S., and Staehling-Hampton, K. (2009) Identification of EMS-induced mutations in Drosophila melanogaster by whole-genome sequencing. *Genetics* **182**, 25–32

42. Solnica-Krezel, L., Schier, A. F., and Driever, W. (1994) Efficient recovery of ENU-induced mutations from the zebrafish germline. *Genetics* **136**, 1401–1420

43. Minevich, G., Park, D. S., Blankenberg, D., Poole, R. J., and Hobert, O. (2012) CloudMap: a cloud-based pipeline for analysis of mutant genome sequences. *Genetics* **192**, 1249–1269

44. Li, H., Handsaker, B., Wysoker, A., Fennell, T., Ruan, J., Homer, N., Marth, G., Abecasis, G., and Durbin, R. (2009) The Sequence Alignment/Map format and SAMtools. *Bioinformatics* **25**, 2078–2079

45. McKenna, A., Hanna, M., Banks, E., Sivachenko, A., Cibulskis, K., Kernytsky, A., Garimella, K., Altshuler, D., Gabriel, S., Daly, M., and DePristo, M. A. (2010) The Genome Analysis Toolkit: a MapReduce framework for analyzing next-generation DNA sequencing data. *Genome Res.* **20**, 1297–1303

46. Bamshad, M. J., Ng, S. B., Bigham, A. W., Tabor, H. K., Emond, M. J., Nickerson, D. A., and Shendure, J. (2011) Exome sequencing as a tool for Mendelian disease gene discovery. *Nat. Rev. Genet.* **12**, 745–755

47. Fairfield, H., Gilbert, G. J., Barter, M., Corrigan, R. R., Curtain, M., Ding, Y., D'Ascenzo, M., Gerhardt, D. J., He, C., Huang, W., Richmond, T., Rowe, L., Probst, F. J., Bergstrom, D. E., Murray, S. A., Bult, C., Richardson, J., Kile, B. T., Gut, I., Hager, J., Sigurdsson, S., Mauceli, E., Di Palma, F., Lindblad-Toh, K., Cunningham, M. L., Cox, T. C., Justice, M. J., Spector, M. S., Lowe, S. W., Albert, T., Donahue, L. R., Jeddeloh, J., Shendure, J., and Reinholdt, L. G. (2011) Mutation discovery in mice by whole exome sequencing. *Genome Biol.* **12**, R86

48. Ryan, S., Willer, J., Marjoram, L., Bagwell, J., Mankiewicz, J., Leshchiner, I., Goessling, W., Bagnat, M., and Katsanis, N. (2013) Rapid identification of kidney cyst mutations by whole exome sequencing in zebrafish. *Development* **140**, 4445–4451

49. Berry, R., and Rodeheffer, M. S. (2013) Characterization of the adipocyte cellular lineage in vivo. *Nat. Cell Biol.* **15**, 302–308

50. Luther, J., Ubieta, K., Hannemann, N., Jimenez, M., Garcia, M., Zech, C., Schett, G., Wagner, E. F., and Bozec, A. (2014) Fra-2/AP-1 controls adipocyte differentiation and survival by regulating PPARgamma and hypoxia. *Cell Death Differ.* **21**, 655–664

51. Magi, A., Tattini, L., Cifola, I., D'Aurizio, R., Benelli, M., Mangano, E., Battaglia, C., Bonora, E., Kurg, A., Seri, M., Magini, P., Giusti, B., Romeo, G., Pippucci, T., De Bellis, G., Abbate, R., and Gensini, G. F. (2013) EXCAVATOR: detecting copy number variants from whole-exome sequencing data. *Genome Biol.* **14**, R120

52. Brown, K. H., Dobrinski, K. P., Lee, A. S., Gokcumen, O., Mills, R. E., Shi, X., Chong, W. W., Chen, J. Y., Yoo, P., David, S., Peterson, S. M., Raj, T., Choy, K. W., Stranger, B. E., Williamson, R. E., Zon, L. I., Freeman, J. L., and Lee, C. (2012) Extensive genetic diversity and substructuring among zebrafish strains revealed through copy number variant analysis. *Proc. Natl. Acad. Sci. U. S. A.* **109**, 529–534

53. Henke, K., Bowen, M. E., and Harris, M. P. (2013) Perspectives for identification of mutations in the zebrafish: making use of next-generation sequencing technologies for forward genetic approaches. *Methods* **62**, 185–196

54. Spalding, K. L., Arner, E., Westermark, P. O., Bernard, S., Buchholz, B. A., Bergmann, O., Blomqvist, L., Hoffstedt, J., Naslund, E., Britton, T., Concha, H., Hassan, M., Ryden, M., Frisen, J., and Arner, P. (2008) Dynamics of fat cell turnover in humans. *Nature* **453**, 783–787

55. Wang, Q. A., Tao, C., Gupta, R. K., and Scherer, P. E. (2013) Tracking adipogenesis during white adipose tissue development, expansion and regeneration. *Nat. Med.* **19**, 1338–1344

56. Grabher, C., and Wittbrodt, J. (2007) Meganuclease and transposon mediated transgenesis in medaka. *Genome Biol.* **8**, S10

57. Suster, M. L., Sumiyama, K., and Kawakami, K. (2009) Transposon-mediated BAC transgenesis in zebrafish and mice. *BMC Genomics* **10**, 477

58. Yang, Z., Jiang, H., Chaichanasakul, T., Gong, S., Yang, X. W., Heintz, N., and Lin, S. (2006) Modified bacterial artificial chromosomes for zebrafish transgenesis. *Methods* **39**, 183–188

59. Zhang, X. Y., and Rodaway, A. R. (2007) SCL-GFP transgenic zebrafish: in vivo imaging of blood and endothelial development and identification of the initial site of definitive hematopoiesis. *Dev. Biol.* **307**, 179–194

60. Kim, H., and Kim, J. S. (2014) A guide to genome engineering with programmable nucleases. *Nat. Rev. Genet.* **15**, 321–334

61. Bibikova, M., Golic, M., Golic, K. G., and Carroll, D. (2002) Targeted chromosomal cleavage and mutagenesis in Drosophila using zinc-finger nucleases. *Genetics* **161**, 1169–1175

62. Li, L., Atef, A., Piatek, A., Ali, Z., Piatek, M., Aouida, M., Sharakuu, A., Mahjoub, A., Wang, G., Khan, S., Fedoroff, N. V., Zhu, J. K., and Mahfouz, M. M. (2013) Characterization and DNA-binding specificities of Ralstonia TAL-like effectors. *Mol. Plant.* **6**, 1318–1330

63. Mak, A. N., Bradley, P., Cernadas, R. A., Bogdanove, A. J., and Stoddard, B. L. (2012) The crystal structure of TAL effector PthXo1 bound to its DNA target. *Science* **335**, 716–719

64. Dahlem, T. J., Hoshijima, K., Jurynec, M. J., Gunther, D., Starker, C. G., Locke, A. S., Weis, A. M., Voytas, D. F., and Grunwald, D. J. (2012) Simple methods for generating and detecting locus-specific mutations induced with TALENs in the zebrafish genome. *PLoS Genet.* **8**, e1002861

65. Zu, Y., Tong, X., Wang, Z., Liu, D., Pan, R., Li, Z., Hu, Y., Luo, Z., Huang, P., Wu, Q., Zhu, Z., Zhang, B., and Lin, S. (2013) TALEN-mediated precise genome modification by homologous recombination in zebrafish. *Nat. Methods.* **10**, 329-331

66. Sommer, D., Peters, A., Wirtz, T., Mai, M., Ackermann, J., Thabet, Y., Schmidt, J., Weighardt, H., Wunderlich, F. T., Degen, J., Schultze, J. L., and Beyer, M. (2014) Efficient genome engineering by targeted homologous recombination in

mouse embryos using transcription activator-like effector nucleases. *Nat. Commun.* **5**, 3045

67. Auer, T. O., and Del Bene, F. (2014) CRISPR/Cas9 and TALEN-mediated knock-in approaches in zebrafish. *Methods* **10**, 682-699

68. Haunerland, N. H., and Spener, F. (2004) Fatty acid-binding proteins--insights from genetic manipulations. *Prog. Lipid Res.* **43**, 328–349

69. Furuhashi, M., and Hotamisligil, G. S. (2008) Fatty acid-binding proteins: role in metabolic diseases and potential as drug targets. *Nat. Rev. Drug Discov.* **7**, 489–503

70. Karanth, S., Denovan-Wright, E. M., Thisse, C., Thisse, B., and Wright, J. M. (2008) The evolutionary relationship between the duplicated copies of the zebrafish fabp11 gene and the tetrapod FABP4, FABP5, FABP8 and FABP9 genes. *FEBS J*. **275**, 3031–3040

71. Kwan, K. M., Fujimoto, E., Grabher, C., Mangum, B. D., Hardy, M. E., Campbell, D. S., Parant, J. M., Yost, H. J., Kanki, J. P., and Chien, C. B. (2007) The Tol2kit: a multisite gateway-based construction kit for Tol2 transposon transgenesis constructs. *Dev. Dyn.* **236**, 3088–3099

72. Sharma, P., Yan, F., Doronina, V. A., Escuin-Ordinas, H., Ryan, M. D., and Brown, J. D. (2012) 2A peptides provide distinct solutions to driving stop-carry on translational recoding. *Nucleic Acids Res.* **40**, 3143–3151

73. Bedell, V. M., Wang, Y., Campbell, J. M., Poshusta, T. L., Starker, C. G., Krug, R. G., 2nd, Tan, W., Penheiter, S. G., Ma, A. C., Leung, A. Y., Fahrenkrug, S. C., Carlson, D. F., Voytas, D. F., Clark, K. J., Essner, J. J., and Ekker, S. C. (2012) In vivo genome editing using a high-efficiency TALEN system. *Nature* **491**, 114–118